SIAM J. APPL. MATH.
Vol. 73, No. 1, pp. 232–253
© 2013 Society for Industrial and Applied Mathematics

Downloaded 03/12/13 to 163.1.237.161. Redistribution subject to SIAM license or copyright; see http://www.siam.org/journals/ojsa.php

EXPONENTIAL ASYMPTOTICS FOR THIN FILM RUPTURE*

S. JONATHAN CHAPMAN†, PHILIPPE H. TRINH†‡, AND THOMAS P. WITELSKI§

Abstract. The formation of singularities in models of many physical systems can be described using self-similar solutions. One particular example is the finite-time rupture of a thin film of viscous fluid which coats a solid substrate. Previous studies have suggested the existence of a discrete, countably infinite number of distinct solutions of the nonlinear differential equation which describes the self-similar behavior. However, no analytical mechanism for determining these solutions was identified. In this paper, we use techniques in exponential asymptotics to construct the analytical selection condition for the infinite sequence of similarity solutions, confirming the conjectures of earlier numerical studies.

Key words. thin film rupture, pinch-off, similarity solutions, exponential asymptotics, beyond-all-orders analysis, Stokes phenomenon

AMS subject classifications. 34E20, 34M40, 35C06, 76A20, 35K25, 34D05

DOI. 10.1137/120872012

1. Introduction.

Previous numerical studies of filament pinch-off and thin film rupture have shown that the formation of such finite-time singularities generally occur in a self-similar manner [15, 16]. In particular, the partial differential equations which model these physical systems admit similarity solutions. By examining the related nonlinear ordinary differential equations for these similarity profiles, previous authors have discovered sets of coexisting solutions; these sets, in many cases, form discrete countably infinite families. Under some conditions, analytical results for existence and stability can be obtained for some problems (see, e.g., section 2.4.1 in [16]), but no general analytical methods have been given that apply to a wide class of nonlinear problems. In this paper, we shall demonstrate how this selection mechanism can be understood using techniques in exponential asymptotics.

The formation of a pinch-off or rupture can occur in a wide range of physical systems (see, for example, reviews by Eggers and coauthors [15, 16, 17], Myers [20], and Oron, Davis, and Bankoff [23]). However, as the singularity is approached, there are only a limited number of possibilities for dominant balances between the different physical effects; the result is that the dynamics tends to be governed by a small number of *universal* scenarios. Four well-known cases which exhibit discrete sets of finite-time similarity solutions include (i) the pinching-off of solids due to surface diffusion by Bernoff, Bertozzi, and Witelski [1]; (ii) the pinching-off of liquid threads due to capillary forces by Brenner, Lister, and Stone [5]; (iii) van der Waals–driven rupture of thin films on solids by Zhang and Lister [35]; and (iv) van der Waals–driven rupture of fluid sheets in free space by Vaynblat, Lister, and Witelski [29, 30]. Problems with analogous self-similar dynamics occur in many other settings [2, 16].

Here we consider the particular case of the simplest model equation for van der

*Received by the editors April 2, 2012; accepted for publication (in revised form) October 5, 2012; published electronically January 29, 2013.
http://www.siam.org/journals/siap/73-1/87201.html
†Oxford Centre for Industrial and Applied Mathematics, Mathematical Institute, University of Oxford, Oxford, Oxfordshire OX1 3LB, UK (chapman@maths.ox.ac.uk).
‡Program in Applied and Computational Mathematics, Princeton University, Princeton, NJ 08544-1000 (ptrinh@princeton.edu).
§Department of Mathematics, Duke University, Durham, NC 27708 (witelski@math.duke.edu).
This author was supported by NSF grant DMS-0968252.

Copyright © by SIAM. Unauthorized reproduction of this article is prohibited.

Downloaded 03/12/13 to 163.1.237.161. Redistribution subject to SIAM license or copyright; see http://www.siam.org/journals/ojsa.php

Waals–driven rupture of a two-dimensional thin film on a solid substrate. Using the most basic expression for the influence of destabilizing intermolecular forces on the film, Williams and Davis [32] proposed a nonlinear evolution equation to model the evolution of the resultant film dynamics, with

$$\frac{\partial h}{\partial t} = -\frac{\partial}{\partial x}\left(\frac{1}{h}\frac{\partial h}{\partial x}\right) - \frac{\partial}{\partial x}\left(h^3 \frac{\partial^3 h}{\partial x^3}\right), \tag{1.1}$$

where $h = h(x,t)$ is the fluid height, given as a function of the spatial coordinate, x, at time t. We assume that as t tends to a critical time t_c, localized rupturing occurs at the point $x = x_c$. This process is depicted in the left frame of Figure 1 using a numerical simulation of (1.1). It was shown by Zhang and Lister [35] that for $t < t_c$, there exist similarity solutions of the form

$$h(x,t) = \tau^{1/5} H(\eta) \quad \text{with} \quad \eta = \left(\frac{x - x_c}{\tau^{2/5}}\right), \tag{1.2}$$

with $\tau = t_c - t$. Thus, the self-similar profiles near rupture are characterized by functions $H(\eta;\epsilon)$, which depend on a similarity variable, η, and are indexed by a far-field scaling parameter, ϵ. By using a numerical shooting method, Zhang and Lister [35] found the first six ($\epsilon \approx 0.651, 0.304, 0.205, 0.156, 0.127, 0.108$) in what appears to be an infinite set of solutions. However, only the first member is stable and observable in direct simulations of the partial differential equation (1.1). Afterwards, these results were confirmed and extended by Witelski and Bernoff [33] using independent numerical schemes and analysis of the stability of the solutions. The principal result of our work is an equation, $\mathcal{F}(n,\epsilon) = 0$, valid for ϵ small, which generates the crucial ϵ that determines each member of the family of self-similar solutions given $n = 1, 2, 3, \ldots$. The first ten of such solutions can be seen in the right frame of Figure 1.

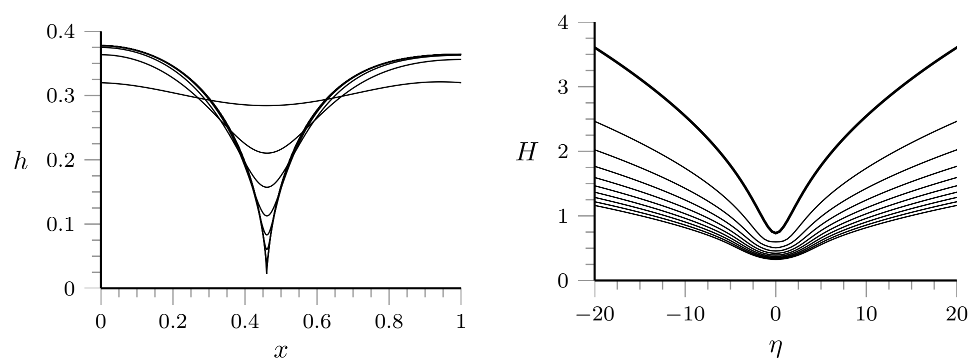

Fig. 1. *(Left) Localized rupture of a thin film modeled using* (1.1) *as the critical time is approached. (Right) The first ten similarity solutions of* (2.1)*, $H(\eta;\epsilon_n)$ with $n = 1$ through* 10*. Only the fundamental solution, with $n = 1$, is linearly stable; here, it is shown in bold.*

The asymptotic limit $\epsilon \to 0$ is singular, and herein lies the chief difficulty: the mechanism which determines which solutions, $H(\eta;\epsilon)$, are admissible crucially depends on exponentially small effects, hidden *beyond all orders* from regular a asymptotic expansion, e.g., $H = H_0 + \epsilon H_1 + \mathcal{O}(\epsilon^2)$; these seemingly inconsequential terms of order $e^{-c/\epsilon}$ for some positive c must be instead studied using *exponential asymptotics*. Similar ideas have been used to derive other selection mechanisms in nature, such as those corresponding to models of viscous fingering [6, 10, 11], crystal growth [19], and vortex reconnection [7].

Copyright © by SIAM. Unauthorized reproduction of this article is prohibited.

Downloaded 03/12/13 to 163.1.237.161. Redistribution subject to SIAM license or copyright; see http://www.siam.org/journals/ojsa.php

In addition to the resolution of the long-standing van der Waals rupture problem, two other significant contributions stem from this work: First, we show how to overcome the challenges that arise in this problem, many of which are not present in previous applications of exponential asymptotics (e.g., in the work of Chapman, King, and Adams [8]). Second, and more importantly, the methodology we develop has wider applicability in regards to other self-similar problems (such as for the pinch-off of solid or liquid filaments); this paper should be seen as the first step towards these future extensions.

2. Mathematical formulation. Substituting the similarity ansatz of (1.2) into the evolution equation (1.1), we see that the similarity solutions satisfy

$$-\frac{1}{5}\Big[H - 2\eta H'\Big] = -\frac{d}{d\eta}\left[\frac{H'}{H}\right] - \frac{d}{d\eta}\Big[H^3 H'''\Big]. \tag{2.1}$$

Here and henceforth, primes ($'$) denote differentiation with respect to the associated variable of the function. Rupturing is a localized behavior, meaning that at any fixed point, x, bounded away from x_c, the evolution of the profile remains essentially uninfluenced by the singularity as $t \to t_c$; this can be expressed as $\partial_t h(x,t) = \mathcal{O}(1)$ away from x_c. Thus, in terms of the rupture solution for $\tau \to 0$, this yields a far-field Robin boundary condition for the self-similar solutions,

$$\frac{1}{5}\Big[H - 2\eta H'\Big] \to 0 \quad \text{as } |\eta| \to \infty,$$

which can be integrated to give the requirement that

$$H(\eta) \sim C|\eta|^{1/2} \quad \text{as } |\eta| \to \infty \tag{2.2}$$

for some positive constant C. Only symmetric solutions of (2.1) have been observed, so we make use of this assumption and solve on the domain $0 \le \eta \le \infty$ with the symmetry conditions $H'(0) = H'''(0) = 0$. Finally, we can normalize the constant C out of the boundary condition (2.2) by rescaling

$$H(\eta) = C^{4/5}\phi(z) \quad \text{and} \quad \eta = C^{-2/5}z, \tag{2.3}$$

thus putting (2.1) into the form

$$\frac{1}{5}\Big[\phi - 2z\phi'\Big] - \frac{d}{dz}\left[\frac{\phi'}{\phi}\right] = \epsilon^2\frac{d}{dz}\Big[\phi^3\phi'''\Big] \tag{2.4a}$$

on $z \in [0,\infty)$, where $\epsilon = C^2$, and with the three boundary conditions

$$\phi'(0) = \phi'''(0) = 0 \quad \text{and} \quad \phi \sim z^{1/2} \text{ as } z \to \infty. \tag{2.4b}$$

The rest of this paper will be devoted to studying problem (2.4a, b).

From numerical work, solutions $\phi = \Phi(z;\epsilon)$ of this problem have been presumed to form the members of a discrete and countably infinite set (see Figure 1). In terms of ϵ, these solutions can then be ordered, with $\Phi(\eta;\epsilon_n)$, where $n = 1, 2, 3, \ldots$, and with values of ϵ_n forming a decreasing sequence. In this paper, we shall be interested in constructing solutions for the limit $\epsilon \to 0$ or, equivalently, as $n \to \infty$.

The source of the problem in solving (2.4) is easily understood: as $z \to \infty$, we can show that solutions contain the following behaviors:

$$\begin{aligned}\phi(z) = \left[z^{\frac{1}{2}} + a_1 z^{\frac{1}{2}} + \mathcal{O}\left(1/z^2\right)\right] &+ a_2 z^{-\frac{1}{3}} e^{-2\beta z^{5/2}} \\ &+ a_3 z^{-\frac{1}{3}} e^{\beta(1+i\sqrt{3})z^{5/6}} + a_4 z^{-\frac{1}{3}} e^{\beta(1-i\sqrt{3})z^{5/6}},\end{aligned} \tag{2.5}$$

Copyright © by SIAM. Unauthorized reproduction of this article is prohibited.

Downloaded 03/12/13 to 163.1.237.161. Redistribution subject to SIAM license or copyright; see http://www.siam.org/journals/ojsa.php

where $\beta = 3[2/(625\epsilon^2)]^{1/3}$. From this equation, we see that in order to satisfy the far-field condition in (2.4b), we need $a_1 = a_3 = a_4 = 0$. However, combined with the two symmetry conditions, this gives a total of five constraints on the solution of a fourth-order equation—the problem is, in fact, overdetermined. This overdeterminancy is a classic sign of a *beyond-all-orders* eigenvalue problem; solutions can only be expected to exist for specific values of ϵ, and this selection mechanism is made clear by using exponential asymptotics.

3. Overview of the general methodology. In studying the rupture problem, we shall encounter four different types of asymptotic expansions, each of which characterizes the different modes that combine to form the final solution:

$$\begin{aligned} &⓪\ \Big[\phi_0(z) + \epsilon\phi_1(z) + \mathcal{O}(\epsilon^2)\Big]e^0, \qquad &&①\ \Big[A_1(z) + \mathcal{O}(\epsilon)\Big]e^{S_1(z)/\epsilon}, \\ &②\ \Big[A_2(z) + \mathcal{O}(\epsilon)\Big]e^{S_2(z)/\epsilon}, &&③\ \Big[A_3(z) + \mathcal{O}(\epsilon)\Big]e^{S_3(z)/\epsilon}. \end{aligned} \tag{3.1}$$

The *base* series, represented by ⓪, is simply the usual expansion for the profile of a thin film near rupture, expressed in terms of its similarity height, ϕ, and coordinate, z, and in powers of the small parameter, ϵ. Qualitatively, this base series is what gives the profile its overall shape. In addition, we find that the problem contains a decaying mode, ①, as well as two exponentially growing modes, ② and ③, which are unbounded in the far field. Our problem, then, is to find values of ϵ for which the contributions from ② and ③ sum to zero at infinity, thus satisfying the boundary conditions. The difficulty, however, is that for all real values of z (describing the *physical* thin film), the base series exponentially dominates the three other contributions—these modes are effectively obscured by the regular perturbation expansion.

In the left frame of Figure 2, we have plotted the first ten solutions, $\phi = \Phi_n$, overlaid with the leading-order approximation from mode ⓪. Although ϕ_0 is a superb approximation throughout, the analytic continuation of the function off the real z-axis contains a series of square-root branch points (Figure 2, right). These singularities will cause the base series ⓪ to diverge on the real axis for any $\epsilon > 0$. In order to

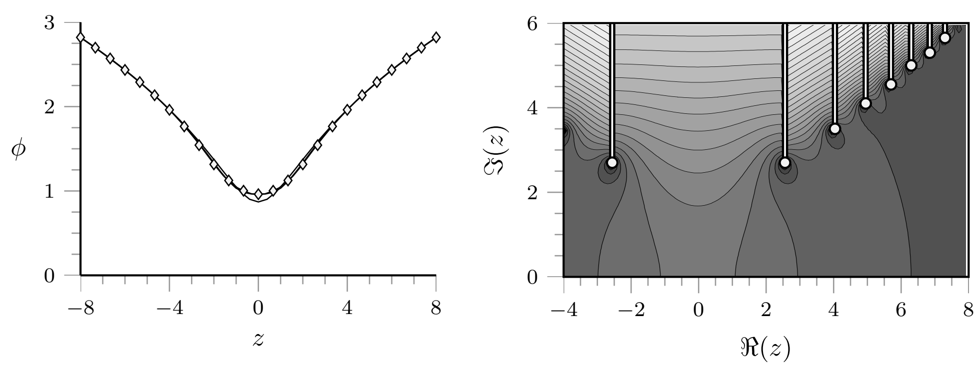

FIG. 2. *(Left) Expressed in terms of ϕ and z using* (2.3)*, the ten similarity solutions of Figure* 1 *(right) closely approach a single curve as n increases. The nodes indicate the leading-order approximation, ϕ_0, derived in section* 4*, which tends to $\sqrt{z}$ as $z \to \infty$. (Right) Contour plot for $|\phi_0(z)|$ with light regions corresponding to small values and dark regions to large values. Crucially, we note the presence of branch points for which the branch cuts are taken directly upwards and shown striped.*

Copyright © by SIAM. Unauthorized reproduction of this article is prohibited.

Downloaded 03/12/13 to 163.1.237.161. Redistribution subject to SIAM license or copyright; see http://www.siam.org/journals/ojsa.php

obtain the best approximation, we can *optimally truncate* the number of terms in ⓪, obtaining an exponentially small remainder.

This remainder obeys an interesting transition: as z is analytically continued across critical curves (*Stokes lines*), ⓪ may *switch on* one of the other modes in a process known as the *Stokes phenomenon.* This rather surprising consequence of singular perturbation theory occupied Stokes at various points [24, 25] throughout his life, and most memorably he described the transition as causing the inferior term to emerge *"as it were into a mist."*

For example, in our problem, we could describe such a transition as

$$\Big[\phi_0 + \mathcal{O}(\epsilon^2)\Big]e^0 \xrightarrow[⓪ > ③]{z^*} \Big[\phi_0 + \mathcal{O}(\epsilon^2)\Big]e^0 + \Big[A_3(x) + \mathcal{O}(\epsilon)\Big]e^{S_3(x)/\epsilon}, \tag{3.2}$$

and the arrow notation should be read as, "⓪ *switches on* ③ *across a Stokes line originating from* z^*." The point z^* is usually a singularity or branch point of the early asymptotic terms (of ⓪ for the above case). The general rules regarding Stokes lines were established by Dingle [14, pp. 6–8] and are as follows: Stokes lines are locations where (i) the two interacting exponentials have equal phase (e.g., $\Im[S_0] = \Im[S_3]$ with $S_0 \equiv 0$); and (ii) the exponential *doing* the switching is larger than the exponential *being* switched (e.g., $-\Re[S_0] \geq -\Re[S_3]$). Together these two conditions imply that at a Stokes line, the exponential doing the switching has reached peak exponential dominance over the other; this is also why we have chosen to use a $>$ sign to mark the process. Of course, it is also possible for other pairs of switchings to occur.

Exponential asymptotics is the name given to the technique of deriving the exponentially small terms switched on by the Stokes phenomenon; its general theory is outlined in the reviews by Boyd [3, 4] and Dingle [14]. The particular methods we shall use, however, stem from Chapman, King, and Adams [8] and Olde Daalhuis et al. [22] and have been applied to a wide variety of problems, particularly in the context of fluid flow [6, 9, 28]. We also note that Stokes lines and the Stokes phenomenon can be studied using other methods such as Borel summation (see, e.g., Grimshaw [18] and Olde Daalhuis [21]). Selection mechanisms which are determined from beyond-all-order terms are also well known, having been studied in models of crystal growth [19], viscous fingering [6, 10, 11, 26, 34], and vortex reconnection [7].

Before turning to the initial asymptotic analysis in the next section, we summarize in Figure 3 some of the key ideas which underlie the asymptotic methodology of the rupturing problem.

4. Initial asymptotic analysis. Let us begin by expanding the solution in terms of a regular perturbation expansion,

$$\phi(z) = \sum_{n=0}^{\infty} \epsilon^n \phi_n(z), \tag{4.1}$$

and substitute the expression into (2.4a) and (2.4b). At leading order, this gives

$$\frac{1}{5}\left[\phi_0 - 2z\phi_0'\right] - \frac{d}{dz}\left[\frac{\phi_0'}{\phi_0}\right] = 0, \tag{4.2}$$

with $\phi_0'(0) = 0$ and $\phi_0 \sim \sqrt{z}$ as $z \to \infty$. The solution of this second-order boundary value for $z \in \mathbb{R}$ can be computed using standard numerical methods, and this process yields the appropriate condition at the origin, with $\phi_0(0) \approx 0.96163849$. Once this

Copyright © by SIAM. Unauthorized reproduction of this article is prohibited.

Downloaded 03/12/13 to 163.1.237.161. Redistribution subject to SIAM license or copyright; see http://www.siam.org/journals/ojsa.php

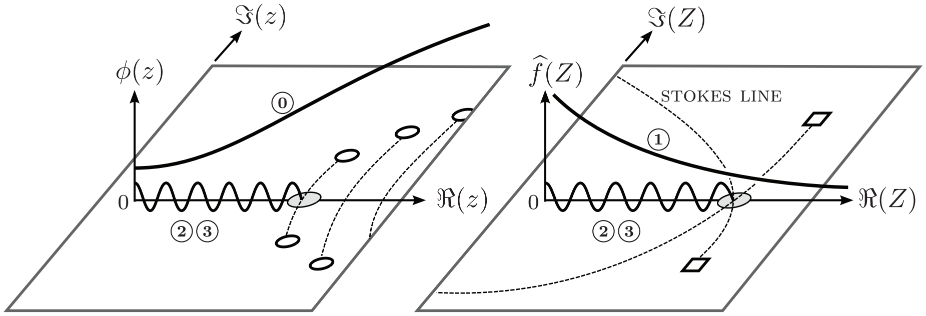

Fig. 3. *(Left) In section* 5*, we show that as the base series,* ⓪*, is analytically continued past the first Stokes line, the two oscillatory modes,* ② *and* ③*, are switched on. These Stokes lines (shown dashed) lie in the complex plane, where $z \in \mathbb{C}$, and originate from singularities (circles). There is an infinitude of such Stokes lines, but we illustrate only the first such switching. (Right) Later in section* 6*, we show that within a far-field scaling, where $Z \gg z$, the decaying mode* ①*, written as $\widehat{f}(Z)$, can also switch on* ② *and* ③ *because of Stokes lines from turning points (squares). Solutions are symmetric (in z), and for a given ϵ, a solution is valid only if the oscillations are switched off at infinity. Ultimately, it is the Stokes phenomenon depicted in the right figure which determines the selection of rupturing solutions.*

initial condition has been obtained, we may integrate the solution to any point in the complex plane.

The modulus, $|\phi_0(z)|$, was previously illustrated in the right frame of Figure 2. In fact, the analytic continuation of the leading-order solution suggests that there exists an infinite set of singularities at the points $z = \sigma_m$ for $m = 1, 2, 3, \ldots$, beginning with $\sigma_1 \approx 2.58 + 2.72i$, and where each of these is a member of a quartet in the complex plane, $\{\sigma_m, -\sigma_m, \overline{\sigma}_m, -\overline{\sigma}_m\}$. The appearance of such nearly periodic arrays of singularities has been shown to be a common trait of self-similar solutions to a wide class of nonlinear partial differential equations (see, e.g., [12, 13]).

In fact, as $m \to \infty$, the locations of the singularities are $|\sigma_m| \sim m^{2/5}$, and this can be derived from the following argument: consider the limit of (4.2) as $|z| \to \infty$; it is straightforward to show that within the first quadrant

$$\phi_0 \sim \left[\sqrt{z} - \frac{1}{2z^2} + \cdots\right] + \left[\frac{C}{z^{4/5}}\right] e^{-\frac{4}{25}z^{5/2}}, \tag{4.3}$$

where the first bracketed terms are found through an algebraic expansion of (4.2), and the exponential is found through a WKB analysis. Later, in section 6.1, we will explain the connection between the unknown constant, C, and the exponentials (3.1) switched on through the Stokes phenomenon.

Notice that the exponential term in (4.3) is exponentially smaller than the algebraic terms for z along the positive real axis, but as z approaches the ray $e^{\pi i/5}$, the exponential factor becomes $\mathcal{O}(1)$. Indeed the singularities, $z = \sigma_m$ as $m \to \infty$, can be found by scaling z such that the first and last terms of (4.3) are balanced. We thus set $z = e^{\pi i/5}(1+s)/\delta$ and assume that both δ and $|s| \ll 1$. A balance of the two terms in (4.3) requires

$$\frac{C\delta^{4/5}}{e^{4\pi i/25}} \exp\left[\left(\frac{4}{25}\right)\left(\frac{5}{2}\right)\frac{\Im(s)}{\delta^{5/2}}\right] \exp\left[-i\left(\frac{4}{25}\right)\frac{1}{\delta^{5/2}}\right] \sim -\frac{e^{\pi i/10}}{\delta^{1/2}},$$

where we have expanded s into its real and imaginary parts in order to isolate the phase contributions of the exponential. On the left-hand side, the second exponential

Copyright © by SIAM. Unauthorized reproduction of this article is prohibited.

only contributes to the oscillations, so in order to ensure similar magnitudes, we choose s so that $\Im(s) \sim -\frac{13}{4}\delta^{5/2}\log\delta$. This motivates us to make the substitution

$$z = \frac{e^{\pi i/5}}{\delta}\left[1 + i\left(-\tfrac{13}{4}\log\delta + \xi\right)\delta^{5/2}\right] \tag{4.4}$$

for the new outer variable, $\xi = \mathcal{O}(1)$. Under this scaling, we can verify that ϕ_0 in (4.3) becomes

$$\phi_0 \sim \frac{e^{\pi i/10}}{\delta^{1/2}}g(\xi), \quad \text{where} \quad g(\xi) \sim g_0 = 1 + C\mu e^{2\Re(\xi)/5}, \tag{4.5}$$

and $\mu = \exp[-4i/(25\delta^{5/2})] = \mathcal{O}(1)$.

Because we are only concerned about the behavior of the singularities of ϕ_0, we are free to approach along any direction of z; consequently without loss of generality we can examine $\xi \in \mathbb{R}$. Equation (4.5) will be used to match the solutions in region where $\xi = \mathcal{O}(1)$.

Returning now to the differential equation for ϕ_0 in (4.2), and using the scalings (4.4) and (4.5), we get for the leading-order problem

$$\frac{2}{5}\frac{dg_0}{d\xi} + \frac{d}{d\xi}\left[\frac{g_0'}{g_0}\right] = 0. \tag{4.6}$$

This equation can be integrated exactly and matched with the outer limit of (4.3) and (4.7) as $\xi \to -\infty$ (or tending towards the real z-axis); this gives

$$g_0 \sim \frac{1}{1 - C\exp[-\frac{4i}{25}\delta^{-5/2}]e^{2\xi/5}}, \tag{4.7}$$

where we note that the prefactor of the real exponential in the denominator is only valid to leading order. From (4.7), we see that within the first quadrant, g has simple poles at

$$\xi_m = \frac{5}{2}\left[-2\pi i m - \log C + \frac{4}{25}\delta^{5/2}\right] \tag{4.8}$$

for $m \in \mathbb{Z}$. Note that within this outer region, we require $\xi_m = \mathcal{O}(1)$, and thus

$$m = \mathcal{O}(\delta^{-5/2}), \tag{4.9}$$

that is to say, along the ray $e^{\pi i/5}$ and in a region located a distance $\mathcal{O}(1/\delta)$ from the origin, we would expect the singularity to be indexed by $\mathcal{O}(\delta^{-5/2})$. Using the scaling for z in (4.4), we then see that the difference between the singularities is $|\sigma_{m+1} - \sigma_m| = \delta^{3/2}|\xi_{m+1} - \xi_m| = \mathcal{O}(\delta^{3/2})$. Solving the recurrence relation and using the connection between m and δ in (4.9), we get the final result of

$$|\sigma_m| = \mathcal{O}(m^{2/5}) \qquad \text{as } m \to \infty. \tag{4.10}$$

This asymptotic result, which establishes the distribution of singularities, is verified in the left frame of Figure 4 in comparison with the numerical computations.

Finally, we also mention that in terms of $\phi_0(z)$, the behavior near the singularities established in (4.7) and (4.8) is simply

$$\phi_0(z) \sim \frac{5}{2\sigma}\left[\frac{1}{z - \sigma_m}\right] \quad \text{as } z \to \sigma_m. \tag{4.11}$$

Copyright © by SIAM. Unauthorized reproduction of this article is prohibited.

Downloaded 03/12/13 to 163.1.237.161. Redistribution subject to SIAM license or copyright; see http://www.siam.org/journals/ojsa.php

Downloaded 03/12/13 to 163.1.237.161. Redistribution subject to SIAM license or copyright; see http://www.siam.org/journals/ojsa.php

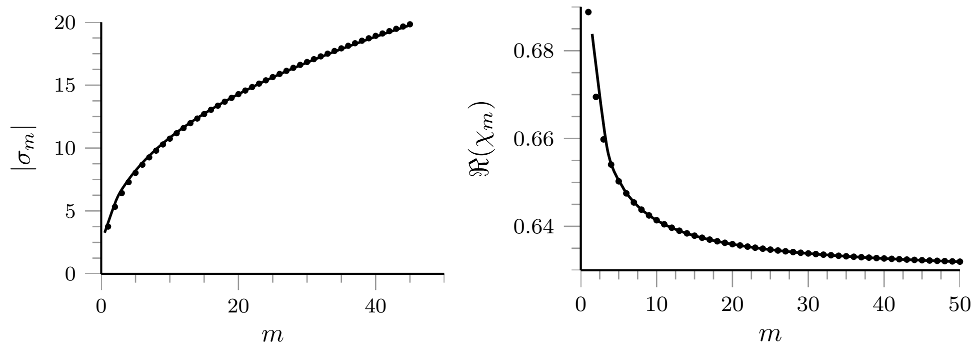

FIG. 4. *(Left) Numerically computed values of* $|\sigma_m|$*, illustrated using dots, with the curve given by the estimate* $4.31m^{2/5}$ *(see* (4.10)*). (Right) Numerically computed values of* $\Re(\chi_m)$*, illustrated using dots, with the curve given the estimate* $0.6279 + 0.0758m^{-3/4}$ *(see* (5.5)*).*

Now if we turn to the higher-order terms of the differential equation (2.4a) using the series in (4.1), we have at $\mathcal{O}(\epsilon^{2n})$ for $n = 1, 2, \ldots$

$$\frac{1}{5}\left[\phi_n - 2z\phi_n'\right] - \frac{d^2}{dz^2}\left[\frac{\phi_n}{\phi_0}\right] = \frac{d}{dz}\left[\phi_0^3\phi_{n-1}'''\right] - \frac{d^2}{dz^2}\left[\frac{\phi_1\phi_{n-1}}{\phi_0^2}\right] + \cdots, \tag{4.12}$$

with the condition that $\phi_n \to 0$ as $z \to \infty$. From this, we see that at each order, ϕ_n is partly determined using the second derivative of ϕ_{n-1}. Thus, each subsequent order necessarily adds 2 the power of the previous singularity, so that in the limit $n \to \infty$, the effects of the early singularities in (4.11) dominate the behavior of the late-order terms. Then for any fixed $z \in \mathbb{R}$, we expect ϕ_n to diverge like a series of factorials over power terms:

$$\phi_n \sim \sum_{m=1}^{\infty} \frac{P_m(z)\Gamma(2n+\gamma_m)}{[\chi_m(z)]^{2n+\gamma_m}} \qquad \text{as } n \to \infty, \tag{4.13}$$

where γ_m is constant. The form of ϕ_n in (4.13) consists of a sum of ansatzes with $\chi_m(\sigma_m) = 0$, and one term for each singularity. We must also add to (4.13) similar terms corresponding to the singularities at $-\sigma_m$, $\overline{\sigma}_m$, and $-\overline{\sigma}_m$. However, because of the linearity of the asymptotic derivation (similar to the process of determining multiple modes in a WKB analysis), we shall dispense with the m-index and examine the terms in (4.13) individually for the moment. Substituting the ansatz into the $\mathcal{O}(\epsilon^n)$ equation (4.12), we find at leading order, as $n \to \infty$, that

$$-\frac{(\chi')^2}{\phi_0} = \phi_0^3(\chi')^4. \tag{4.14}$$

Ignoring the trivial solution, we have $\chi' = \pm i\phi_0^2$ or, selecting the positive branch without loss of generality,

$$\chi(z) = i\int_{\sigma}^{z} \frac{1}{\phi_0^2}\,dt. \tag{4.15}$$

Copyright © by SIAM. Unauthorized reproduction of this article is prohibited.

Downloaded 03/12/13 to 163.1.237.161. Redistribution subject to SIAM license or copyright; see http://www.siam.org/journals/ojsa.php

Continuing to the next order as $n \to \infty$, we determine $P = P_m$ by

$$\frac{z}{5}\Big[2\chi' P\Big] + \frac{1}{\phi_0}\Big[2\chi' P' + \chi'' P\Big] - \frac{\phi_0'}{\phi_0^2}\Big[2\chi' P\Big] = -\phi_0^3\Big[4(\chi')^3 P' + 6\chi''(\chi')^2 P\Big] - \phi_0^2\phi_0'\Big[3(\chi')^3 P\Big], \tag{4.16}$$

or simply

$$\frac{P'}{P} = \frac{z\phi_0}{5} - \frac{5\phi_0'}{2\phi_0} - \frac{5\chi''}{2\chi'}, \tag{4.17}$$

so that, upon using (4.14), P is given by

$$P(z) = \Lambda \phi_0^{5/2} \exp\left(\int_s^z \frac{t\phi_0}{5}\, dt\right), \tag{4.18}$$

where Λ is a constant and s is arbitrary. Thus, each singularity $\sigma = \sigma_m$ is associated with a singulant $\chi = \chi_m$ from (4.15) and prefactor $P = P_m$ from (4.18). The remaining constants (γ_m and Λ_m) which appear in (4.13) and (4.18) can be determined by matching inner and outer solutions near the singularities, σ_m; for the purpose of this work, however, their exact values are not needed. In the next section, we shall discuss the connection between the late terms, ϕ_n, and the Stokes phenomenon.

5. Stokes phenomenon in the $\mathcal{O}(1)$ scaling. The underlying divergence of the asymptotic expansion ⓪ in (4.1) causes the Stokes phenomenon to occur: as the complexified solution crosses critical curves (Stokes lines) which originate from each of the singularities, σ_m, it switches on a subdominant exponential. Before we examine these Stokes lines, however, let us review how the exponentials can be derived. First, we truncate the base series (4.1), writing

$$\phi(z) = \sum_{n=0}^{N-1} \epsilon^{2n}\phi_n(z) + R_N(z). \tag{5.1}$$

Next, we substitute this expression into the differential equation (2.4a), giving a linear equation for the remainder:

$$\frac{1}{5}\Big[R_N - 2zR_N'\Big] - \frac{d^2}{dz^2}\left[\frac{R_N}{\phi_0}\right] - \epsilon^2\frac{d}{dz}\Big[\phi_0^3 R_N'''\Big] + \epsilon^2\frac{d^2}{dz^2}\left[\frac{\phi_1}{\phi_0}R_N\right] \sim \epsilon^{2N}\frac{d}{dz}\Big[\phi_0^3\phi_{N-1}'''\Big]. \tag{5.2}$$

The result, (5.2), expresses the fact that the remainder, R_N, is typically $\mathcal{O}(\epsilon^{2N})$, and hence only algebraically small; however, if N is chosen to be the *optimal truncation point*, then R_N becomes *exponentially small*—this exponentially small error, in fact, simply corresponds to the hidden modes, ② and ③, which lie beyond all orders. Moreover, since the optimal truncation point, $N \to \infty$ as $\epsilon \to 0$, this shows us that R_N is determined using the late terms in (4.13). This process of optimally truncating, and then examining R_N as the Stokes line is crossed, has been shown in [22] and [27], and the steps are generically similar here as well, so we do not repeat them.

Copyright © by SIAM. Unauthorized reproduction of this article is prohibited.

Downloaded 03/12/13 to 163.1.237.161. Redistribution subject to SIAM license or copyright; see http://www.siam.org/journals/ojsa.php

The final result is the following: As the Stokes line from σ_m is crossed, the base series, ⓪, switches on an exponential of the form

$$\left[\phi_0 + \epsilon\phi_1 + \cdots\right] e^0 \xrightarrow[\text{⓪} > \text{②}, \text{③}]{\sigma_m} \left[\phi_0 + \epsilon\phi_1 + \cdots\right] e^0 + \frac{2\pi i}{\epsilon^{\gamma_m}} P_m e^{\pm\chi_m/\epsilon}. \tag{5.3}$$

In (5.3), we have chosen to assign ② to $e^{\chi/\epsilon}$ and ③ to $e^{-\chi/\epsilon}$. The arrow notation indicates the singularity responsible for the Stokes line (σ_m), as well as the switching process.

The more important question, however, is *where are these transitions occurring*? From Dingle [14], Stokes lines, where ⓪ switches on ②, are given by $\Im(\chi_m) = 0$ and $\Re(\chi_m) > 0$; similarly, ⓪ will switch on ③ wherever $\Im(-\chi_m) = 0$ and $\Re(-\chi_m) > 0$. The requirements on the imaginary parts express the fact that Stokes lines are equal phase lines, whereas the requirements on the real parts express the fact that at Stokes lines, the magnitude of ⓪ reaches peak dominance over the other modes; thus we may write ⓪ > ②, ③. Also important are the *anti-Stokes lines*, where the exponentials are of comparable size; these are simply given by $\Re(\chi_m) = 0$.

Each singularity, in fact, generates three Stokes lines and six anti-Stokes lines. However, we are primarily concerned with the physical thin film problem and the boundary conditions in (2.4b), so the only relevant Stokes lines are the ones that intersect the real axis. The result is shown in Figure 5. Observe the surprising arrangement of anti-Stokes lines: Each singularity, σ_m for $m \geq 1$, produces an anti-Stokes line which lies closer to the real axis than the corresponding line from σ_{m-1}. Along the real axis, $\Re(\chi_m)$ is constant, so it must be the case that

$$\Re(\chi_1) > \Re(\chi_2) > \Re(\chi_3) > \cdots \tag{5.4}$$

for $z \in \mathbb{R}$. For a typical problem in exponential asymptotics, the dominant exponential is related to the nearest singularity from the domain which was analytically continued. We would have thus expected that, near the origin, the beyond-all-orders behavior is determined using $\{\sigma_1, -\sigma_1, \overline{\sigma}_1, -\overline{\sigma}_1\}$. For the rupturing problem, however, we see that this is not the case, and the dominant exponential is generated near $z = \infty$.

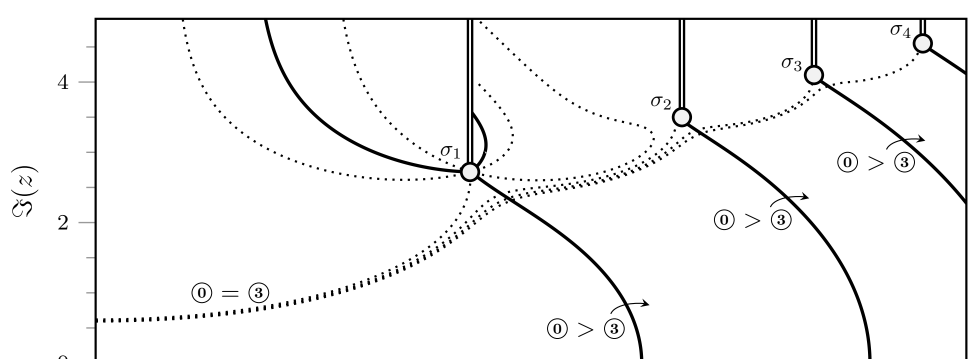

FIG. 5. *Stokes (solid) and anti-Stokes (dotted) lines, originating from the $z = \sigma_m$ singularities. For σ_1, all three Stokes lines and all six anti-Stokes lines are shown; for the others, only the important Stokes and anti-Stokes lines are shown. The key observation is that along the real axis, the exponentials generated by each subsequent singularity (m increasing) dominate the previous ones.*

Copyright © by SIAM. Unauthorized reproduction of this article is prohibited.

Downloaded 03/12/13 to 163.1.237.161. Redistribution subject to SIAM license or copyright; see http://www.siam.org/journals/ojsa.php

Numerically we find that as $m \to \infty$,

$$\Re(\chi_m) \sim b + cm^{-3/4}, \tag{5.5}$$

where $b \approx 0.6279$ and $c \approx 0.0758$ (see the right frame of Figure 4), while the spacing between singularities, $\sigma_{m+1} - \sigma_m = \mathcal{O}(m^{-3/5})$, is given by (4.10). Thus the difference between successive exponentials is getting smaller, and the Stokes lines are getting closer together, as $m \to \infty$. This is all indicative of the existence of another asymptotic region in the far field. In the next section we examine this far-field region by rescaling near infinity and examining the problem there.

6. Stokes phenomenon in the far-field scaling. Let us rescale the equations in (2.4), so that we may examine the solution near $z = \infty$. We write $z = \epsilon^{-2/5} Z$ and $\phi = \epsilon^{-1/5} f$, and this gives

$$\frac{1}{5}\left[f - 2Zf'\right] - \epsilon \frac{d}{dZ}\left[\frac{f'}{f}\right] - \epsilon^3 \frac{d}{dZ}\left[f^3 f'''\right] = 0, \tag{6.1}$$

with the boundary condition $f \sim \sqrt{Z}$ as $|Z| \to \infty$. Appealing to symmetry, we shall again work with analytic continuation of the ordinary differential equation (6.1) from $Z \in \mathbb{R}^+$ for the rest of this section. As in section 4, we can expand the solution as $f = \sum \epsilon^n f_n$, and this gives

$$f \sim f_* = Z^{\frac{1}{2}} - \frac{\epsilon}{2Z^2} - \frac{35\epsilon^2}{16 Z^{\frac{9}{2}}} + \mathcal{O}(\epsilon^3), \tag{6.2}$$

or, simply, the far-field behavior of the unscaled series in (4.1) as $z \to \infty$. In addition to this, we have three possible types of WKB behavior. If we linearize about the expansion (6.2) and write $f = f_* + \widehat{f}$ in (6.1), then we have

$$\frac{1}{5}\left[\widehat{f} - 2\widehat{f}'\right] - \epsilon \frac{d}{dZ}\left[\frac{\widehat{f}'}{f_*} - \frac{f_*'}{f_*^2}\widehat{f}\right] - \epsilon^3 \frac{d}{dZ}\left[f_*^3 \widehat{f}''' + 3f_*^2 f_*''' \widehat{f}\right]. \tag{6.3}$$

Writing the solution as $\widehat{f} = A(Z)e^{S(Z)/\epsilon}$, we find at leading order the eikonal equation

$$-\frac{2}{5} Z S' - Z^{-\frac{1}{2}} (S')^2 - Z^{\frac{3}{2}} (S')^4 = 0. \tag{6.4}$$

The trivial solution $S' = 0$ simply corresponds to the algebraic mode, i.e., the a_1 term in (2.5), and this mode must be eliminated in order to satisfy the boundary conditions. The other three modes are obtained as roots of the cubic equation:

$$S_1'(Z) = -\left(\frac{5}{3}\right)^{\frac{1}{3}} \frac{1}{\beta^{\frac{1}{3}}} + \frac{\beta^{\frac{1}{3}}}{(45)^{\frac{1}{3}} Z^2}, \tag{6.5a}$$

$$S_{2,3}'(Z) = \left(\frac{5}{3}\right)^{\frac{1}{3}} \frac{(1 \pm i\sqrt{3})}{2\beta^{\frac{1}{3}}} - \frac{(1 \mp i\sqrt{3})\beta^{\frac{1}{3}}}{2(45)^{\frac{1}{3}} Z^2}, \tag{6.5b}$$

where β is given by

$$\beta = -9Z^{\frac{11}{2}} + \sqrt{3} Z^3 \sqrt{25 + 27Z^5} = -9Z^{\frac{11}{2}} + 9Z^3 \prod_{k=0}^{4} \sqrt{Z - Z_k}, \tag{6.6}$$

Copyright © by SIAM. Unauthorized reproduction of this article is prohibited.

Downloaded 03/12/13 to 163.1.237.161. Redistribution subject to SIAM license or copyright; see http://www.siam.org/journals/ojsa.php

with $Z_k = (25/27)^{1/5} e^{(2k+1)\pi i/5}$ denoting the *turning points*. We thus have the expressions

$$S_{j,k}(Z) = \int_{Z_k}^{Z} S_j'(t)\, dt, \tag{6.7}$$

which, for $j = 1, 2, 3$, simply correspond to the far-field representations of our three WKB solutions ①, ②, and ③, integrated from each of the five turning points.

At next order, (6.3) yields the amplitude equation

$$10Z^{\frac{5}{2}} A' \left[-3Z^{\frac{3}{2}} - 10S' + 9Z^{\frac{7}{2}} (S')^2 \right] + A \left[78Z^3 + 215Z^{\frac{3}{2}} S' + 10(10 + 3Z^5)(S')^2 \right] = 0, \tag{6.8}$$

from which we gather that

$$A_j = B_j \exp \left(- \int_s^Z G(t; S_j')\, dt \right) \tag{6.9}$$

for $j = 1, 2, 3$, where B_j is constant, where s may be chosen arbitrarily, and where we have defined

$$G(t; S') \equiv \frac{78t^3 + 215t^{\frac{3}{2}} S'(t) + 10(10 + 3t^5)(S'(t))^2}{10t^{\frac{5}{2}} \{ -3t^{\frac{3}{2}} - 10S'(t) + 9t^{\frac{7}{2}} [S'(t)]^2 \}}. \tag{6.10}$$

The three WKB solutions, ①, ②, and ③, which have amplitudes and powers given by (6.7) and (6.9), are connected at the *turning points* $Z = Z_k$ corresponding to locations where the eikonal equation (6.4) has a double root for S'. In Appendix A, we will show that at the kth turning point, two of the three WKB solutions are then scaled like Airy functions, with

$$\text{ⓘ and ⓙ} \sim \left[\frac{\text{const.}}{(Z - Z_k)^{1/4}} \right] \times e^{\pm \text{const.} \times (Z - Z_k)^{3/2}/\epsilon}, \tag{6.11}$$

and $i, j = 1, 2, 3$, and the positive and negative signs, respectively, assigned to ⓘ and ⓙ (or vice versa). The important observation from (6.11) is that it is possible for one exponential to switch on its pair across a Stokes line originating from Z_k; these lines are given by points $Z \in \mathbb{C}$, where

$$\Im \left[\int_{Z_k}^{Z} (S_i' - S_j')\, dt \right] = 0 \quad \text{and} \quad \Re \left[\int_{Z_k}^{Z} (S_i' - S_j')\, dt \right] > 0, \tag{6.12}$$

where $i, j = 1, 2, 3$ and $k = 0, 1, \ldots, 4$. Equation (6.12) gives the prescription of the Stokes line which originates from Z_k and corresponds to $e^{S_i/\epsilon}$ switching on $e^{S_j/\epsilon}$, or simply ⓘ > ⓙ. In Appendix B, we will show how these Stokes lines can be computed.

We now turn to Figure 6, where we have plotted the five turning points and their associated Stokes lines in the Z-plane, but where the figure is only applicable for analytic continuation from $Z \in \mathbb{R}^+$. The important transition occurs as Z is analytically continued across $Z \approx 0.7$; here, ① switches on ③ crossing the Stokes line from Z_0, and ① switches on ② crossing the Stokes line from Z_1. This is the crucial process, and the ② and ③ exponentials switched on will determine the selection mechanism for rupturing.

Copyright © by SIAM. Unauthorized reproduction of this article is prohibited.

Downloaded 03/12/13 to 163.1.237.161. Redistribution subject to SIAM license or copyright; see http://www.siam.org/journals/ojsa.php

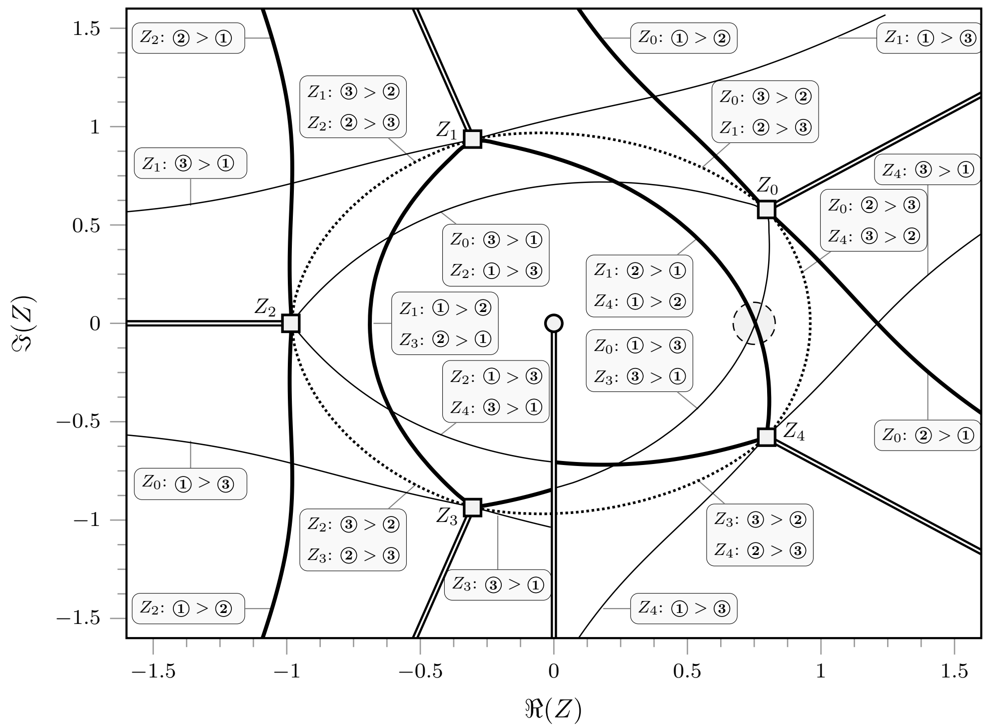

FIG. 6. *Stokes lines from the five turning points in the far-field scaling, applicable for when the original problem is analytically continued to $\Re(Z) > 0$; when $\Re(Z) < 0$, the figure should be reflected about the imaginary axis. Lines for interactions between ① and ② are thick, between ① and ③ are thin, and between ② and ③ are dotted. Branch cuts are shown striped. The circled intersection point is a crucial component in our analysis.*

6.1. The selection mechanism. To complete the solution and determine the selection mechanism we need to match the far-field solution, f, to the near-field solution, ϕ. Recall from (4.3) that

$$\phi_0 \sim \left[\sqrt{z} - \frac{1}{2}z^{-2} + \cdots\right] + Cz^{-4/5}e^{-\frac{4}{25}z^{5/2}}. \tag{6.13}$$

A simple check of the local behavior of $S_1(Z)$ as $Z \to 0$ shows that

$$CZ^{-4/5}e^{-\frac{4}{25}Z^{5/2}} \sim A_1 e^{S_1(Z)/\epsilon}, \tag{6.14}$$

so that this decaying exponential from the near-field region matches with WKB solution ① in the far field. The constant C which determines the amplitude of the decaying mode can be numerically computed; however, its exact value will turn out to be unimportant. To this mode we must add the (exponentially small) contribution from the two oscillating exponentials $e^{\pm\chi/\epsilon}$ generated by all the Stokes lines in the near-field region; these oscillating exponentials then match with the two WKB solutions given by ② and ③.

The key remaining step is to derive the form of the switchings which occur when the WKB mode ① crosses the two key Stokes lines in Figure 6; this involves some laborious algebra, which we postpone until Appendix A. The result, however, is that

Copyright © by SIAM. Unauthorized reproduction of this article is prohibited.

Downloaded 03/12/13 to 163.1.237.161. Redistribution subject to SIAM license or copyright; see http://www.siam.org/journals/ojsa.php

upon crossing the Stokes line from Z_0, the decaying mode switches on a multiple of the WKB solution ③, which (anticipating the matching to follow), we write in terms of the inner variable z as

$$\left[\frac{C}{z^{4/5}}\right] e^{-\frac{4}{25}z^{5/2}} \xrightarrow[\text{①} > \text{③}]{Z_0} \left[\frac{C}{z^{4/5}}\right] e^{-\frac{4}{25}z^{5/2}} + \lambda\epsilon^{39/50} \exp\left[-\frac{2i\log\epsilon}{5\epsilon} + \frac{b}{\epsilon}\right] \times \phi_0^{5/2}(z) \exp\left[\int_s^x \frac{t\phi_0}{5}\,dt\right] \exp\left[-\frac{i}{\epsilon}\int_s^x \frac{1}{\phi_0^2}\,dt\right]; \tag{6.15}$$

here s can be chosen without loss of generality to be real and positive, and λ and b are constants given by (A.20) and (A.19). This exponential cannot be present at infinity, and therefore must be switched on to the left of Z_0. Matching with the near-field solution implies that this is the amplitude of the oscillatory exponential as $z \to \infty$. Now as we cross all the Stokes lines in the inner region this amplitude will be altered. However, it turns out that the sum of all these Stokes jumps is still exponentially small: the Stokes lines in the near-field region are all subdominant to that in the far-field region.

To see this, recall from (4.10) and (5.5) that $\sigma_m = \mathcal{O}(m^{2/5})$ and $\Re(\chi_m) \sim b + cm^{-3/4}$ as $m \to \infty$. When we have gone to the outer region, with $z = \mathcal{O}(\epsilon^{-2/5})$, this means that we have reached index values of $m = \mathcal{O}(\epsilon^{-1})$. Thus, we have

$$\frac{\Re(\chi_m)}{\epsilon} = \frac{b}{\epsilon} + \mathcal{O}(\epsilon^{-1/4}).$$

Since the exponential switched on in the far-field region is $\mathcal{O}(e^{-b/\epsilon})$, the inner switchings are exponentially subdominant by a factor $\mathcal{O}(\exp(-\epsilon^{-1/4}))$. Thus we are able to conclude that the exponential in (6.15) is essentially unchanged all the way to the origin.

There is a similar switching from the ① > ② transition due to the Stokes line from Z_4; this simply results in the complex conjugate of the switching in (6.15). Thus, if we write $\lambda = |\lambda|e^{i\Psi}$, then for $z \in \mathbb{R}^+$ the combined contribution from the ② and ③ exponentials are given by

$$\sim \left[\frac{2|\lambda|\exp(\frac{\Re(b)}{\epsilon} + \int_s^z \frac{t\phi_0}{5}\,dt)}{\epsilon^{-39/50}\phi_0^{-5/2}}\right] \cos\left[\Psi - \frac{2\log\epsilon}{5\epsilon} + \frac{\Im(b)}{\epsilon} - \frac{1}{\epsilon}\int_s^0 \frac{1}{\phi_0^2}\,dt\right]. \tag{6.16}$$

From the boundary condition (2.4b), we need to impose that the third derivative of (6.16) is zero at the origin; to leading order, this gives the requirement that

$$\sin\left[\Psi - \frac{2\log\epsilon}{5\epsilon} + \frac{\Im(b)}{\epsilon} - \frac{1}{\epsilon}\int_s^0 \frac{1}{\phi_0^2}\,dt\right] = 0, \tag{6.17}$$

or that

$$\mathcal{F}(n,\epsilon) \equiv \Psi - \frac{2\log\epsilon}{5\epsilon} + \frac{\Im(b)}{\epsilon} - \frac{1}{\epsilon}\int_s^0 \frac{1}{\phi_0^2}\,dt - n\pi + \pi = 0 \tag{6.18}$$

for $n \in \mathbb{Z}^+$. The π term shifts n so that the first valid solution begins at $n = 1$. The derivation of $\mathcal{F}(n,\epsilon)$ is now complete. In Appendix A, we show that when $s = 1$, then $\Psi \approx -2.7393$, $\Im(b) \approx -0.1486$, and the integral ≈ -1.0176. The result is shown in Figure 7. The fit between the asymptotic prediction and numerical computation is excellent.

Copyright © by SIAM. Unauthorized reproduction of this article is prohibited.

Downloaded 03/12/13 to 163.1.237.161. Redistribution subject to SIAM license or copyright; see http://www.siam.org/journals/ojsa.php

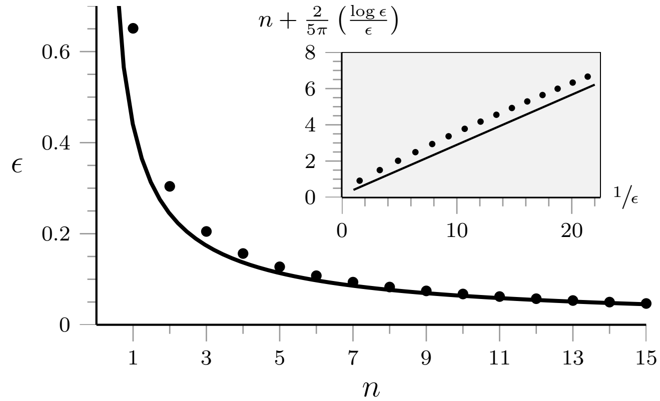

Numerical	Asymptotic
0.651071	0.437836
0.303993	0.243774
0.204949	0.173874
0.156492	0.136843
0.127355	0.113616
0.107764	0.097569
0.093626	0.085761
0.082911	0.076677
0.074422	0.069454
0.067625	0.063562
0.062005	0.058656
0.057287	0.054503
0.053277	0.050938
0.049800	0.047842
0.046760	0.045125

FIG. 7. *The large figure shows the asymptotic (solid) versus numerical (dotted) predictions for the first* 15 *solutions of the rupturing problem; values of* ϵ *are also listed in the table. Within the smaller inset, the asymptotics correctly predict that condition* (6.18) *is satisfied for* $1/\epsilon$ *large.*

7. Discussion. On the most basic level, the derivation of the selection mechanism, $\mathcal{F}(n, \epsilon) = 0$, which applies for the case of van der Waals–driven rupture of a thin film, involves the same key ideas as for other classic beyond-all-orders selection problems: the common theme throughout is the exclusion of exponentially small oscillations, switched on via the Stokes phenomenon, in order to satisfy a set of overdetermined boundary conditions.

However, our problem contains a variety of new difficulties not encountered in previous exponential asymptotic studies. Let us highlight three significant obstacles: (i) the leading-order solution, ϕ_0, which contains the necessary singularity information, can only be determined numerically; (ii) the exponentials, ② and ③, relevant to the selection mechanism, were not switched on by any finite singularity, $\sigma = \sigma_m$, but rather by a clustering of such singularities at infinity; and (iii) the asymptotic series, ①, which performs the key switching is a decaying mode in the leading-order solution—thus, the selection mechanism is determined by a *doubly* small exponential (as opposed to a singly small switching due to the base series, ⓪).

Finally, while our analysis was carried out for the particular case of two-dimensional rupture due to attractive van der Waals forces, the mathematics of pinch-off and rupturing due to other physical mechanisms share similar characteristics to our own. Thus, it appears likely that the resolution of these other selection problems will involve analogous techniques to the ones we have developed here. Work on these and other extensions is ongoing.

Appendix A. Matching of turning-point solutions. In this section, we derive the form of the ① > ③ switching which occurs when the decaying mode is analytically continued past the Stokes line from $Z_0 = (25/27)^{1/5} e^{\pi i/5}$; our task will culminate with the derivation of (6.15). There is a similar switching with ① > ② from the Z_4-Stokes line, and this simply yields the complex conjugate of our result.

First, let us examine Table 1, which contains a list of the local behaviors of S_j' near $Z = 0$, $Z = Z_0$, and $Z = \infty$. Remarking that the values of A_j in (6.9) are unbounded as the origin or turning point is approached, we can add and subtract the

Copyright © by SIAM. Unauthorized reproduction of this article is prohibited.

Table 1

Asymptotic behavior of the three exponents from (6.5a) *and* (6.5b), *where* $W = Z - Z_0$. *Note that of the three exponentials given by the expression* $\exp(S_j'/\epsilon)$ *for* $j = 1, 2, 3$, *only* ① *decays at infinity, so it must be the case that the amplitudes of* ② *and* ③ *vanish in the far field.*

$S_1'(Z \to 0)$	$\sim$	$\left[-\frac{2}{5}\right] Z^{\frac{3}{2}}$	$+$	$\left[\frac{8}{125}\right] Z^{\frac{13}{2}}$	$+$	$\mathcal{O}(Z^{\frac{23}{2}})$
$S_{2,3}'(Z \to 0)$	$\sim$	$\left[\pm i\right] Z^{-1}$	$+$	$\left[\frac{1}{5}\right] Z^{\frac{3}{2}}$	$+$	$\mathcal{O}(Z^4)$
$S_{1,3}'(Z \to Z_0)$	$\sim$	$\left[\left(\frac{2e^{-7\pi i}}{5^4}\right)^{\frac{1}{10}}\right]$	$\pm$	$\left[\left(\frac{e^{7\pi i}}{15}\right)^{\frac{1}{10}}\right] W^{\frac{1}{2}}$	$+$	$\mathcal{O}(W^{\frac{3}{2}})$
$S_2'(Z \to Z_0)$	$\sim$	$\left[2\left(\frac{3e^{3\pi i}}{5^4}\right)^{\frac{1}{10}}\right]$	$+$	$\left[\frac{13}{3}\left(\frac{e^{11\pi i}}{3^3 5^8}\right)^{\frac{1}{10}}\right] W$	$+$	$\mathcal{O}(W^2)$
$S_1'(Z \to \infty)$	$\sim$			$\left[-\left(\frac{2}{5}\right)^{\frac{1}{3}}\right] Z^{-\frac{1}{6}}$	$+$	$\mathcal{O}(Z^{-\frac{11}{6}})$
$S_{2,3}'(Z \to \infty)$	$\sim$			$\left[\left(\frac{1}{20}\right)^{\frac{1}{3}}(1 \pm \sqrt{3}i)\right] Z^{-\frac{1}{6}}$	$+$	$\mathcal{O}(Z^{-\frac{11}{6}})$

local behaviors from the integrand to ease the matching procedure, writing

$$A_1 = \left[\frac{B_1}{(Z - Z_0)^{1/4} Z^{4/5}}\right] \exp\left[-\int_s^Z \mathcal{G}_1(t)\ dt\right], \tag{A.1}$$

$$A_3 = \left[\frac{B_3 Z^{23/20} e^{\frac{2}{5} i Z^{5/2}}}{(Z - Z_0)^{1/4}}\right] \exp\left[-\int_s^Z \mathcal{G}_3(t)\ dt\right], \tag{A.2}$$

where we have defined

$$\mathcal{G}_1(t) \equiv G(t; \phi_1) - \frac{1}{4(t - X_0)} - \frac{4}{5t}, \tag{A.3}$$

$$\mathcal{G}_3(t) \equiv G(t; \phi_3) - \frac{1}{4(t - X_0)} - \frac{i}{t^{7/2}} + \frac{23}{20t}, \tag{A.4}$$

so that both $\mathcal{G}_1$ and $\mathcal{G}_3$ are integrable at $Z = 0$ and $Z = \infty$.

We are now in a position to calculate the solution in the outer region. First, we match the far-field behavior of ϕ_0 with the WKB solution using (6.14) and (A.1). This gives a relation between B_1 and C:

$$B_1 = C(-Z_0)^{1/4} \exp\left[\int_s^0 \mathcal{G}_1(t)\, dt\right] \exp\left[-\frac{1}{\epsilon}\int_{Z_0}^0 \left(S_1' + \frac{4}{25} t^{5/2}\right) dt\right]. \tag{A.5}$$

Let us also introduce constants p and q:

$$p \equiv \left(\frac{3e^{-7\pi i}}{5^4}\right)^{1/10} \qquad \text{and} \qquad q \equiv \frac{2}{3}\left(\frac{e^{-3\pi i}}{15}\right)^{1/10}. \tag{A.6}$$

As we approach the turning point, with $Z = Z_0 + \epsilon^{2/3}\xi$, the first WKB solution gives

$$A_1 e^{S_1/\epsilon} \sim \left[\exp\left(\frac{p\xi}{\epsilon^{1/3}}\right) \frac{B_1 \exp\left(-\int_s^{Z_0} \mathcal{G}_1\, dt\right)}{\epsilon^{1/6} Z_0^{4/5}}\right] \times \frac{e^{-q\xi^{3/2}}}{\xi^{1/4}}, \tag{A.7}$$

while the third WKB solution tends to

$$A_3 e^{S_3/\epsilon} \sim \left[\exp\left(\frac{p\xi}{\epsilon^{1/3}}\right) \frac{B_3 \exp\left(-\int_s^{Z_0} \mathcal{G}_3\, dt\right) \exp\left(\frac{2i}{5} Z_0^{-5/2}\right)}{\epsilon^{1/6} Z_0^{-23/20}}\right] \times \frac{e^{q\xi^{3/2}}}{\xi^{1/4}}. \tag{A.8}$$

Copyright © by SIAM. Unauthorized reproduction of this article is prohibited.

Downloaded 03/12/13 to 163.1.237.161. Redistribution subject to SIAM license or copyright; see http://www.siam.org/journals/ojsa.php

Downloaded 03/12/13 to 163.1.237.161. Redistribution subject to SIAM license or copyright; see http://www.siam.org/journals/ojsa.php

If we like, we can rescale f and Z near $Z = Z_0$, with the intention of removing the square-bracketed prefactors of (A.7) and (A.8). The equation for f and Z in (6.1) would then reduce to an Airy equation, for which we can perform the local Stokes-line analysis. However, it is faster to observe that near the turning point, the typical Airy-like switching requires

$$\frac{e^{-q\xi^{3/2}}}{\xi^{1/4}} \xrightarrow[\text{①} > \text{③}]{Z_0} \frac{e^{-q\xi^{3/2}}}{\xi^{1/4}} + i\,\frac{e^{q\xi^{3/2}}}{\xi^{1/4}}, \tag{A.9}$$

or that, in words, the dominant exponential switches on the subdominant exponential with a prefactor equal to i (see, e.g., section 5.2 in [31]). Using (A.7) to (A.9), we find that the relation between B_1 and B_3 is

$$\frac{iB_1}{Z_0^{4/5}} \exp\left(-\int_s^{Z_0} \mathcal{G}_1\, dt\right) = \frac{B_3}{Z_0^{-23/20}} \exp\left(\frac{2i}{5Z_0^{5/2}}\right) \exp\left(-\int_s^{Z_0} \mathcal{G}_3\, dt\right), \tag{A.10}$$

or, writing B_1 in terms of C from (A.5), that

$$\begin{aligned} B_3 = \frac{e^{\pi i/4}\epsilon^{8/25} C}{Z_0^{17/10}} &\exp\left(-\frac{2i}{5Z_0^{5/2}} - \frac{1}{\epsilon}\int_{Z_0}^0 S_1'\, dt\right) \\ &\times \exp\left(\int_s^{Z_0} \mathcal{G}_3\, dt\right) \exp\left(\int_{Z_0}^0 \mathcal{G}_1\, dt\right). \end{aligned} \tag{A.11}$$

This completely determines the form of ③, which is switched on by ① (specified by a prefactor, C). The last step is to rewrite this result in terms of inner-region variables. Within the inner region, the exponentials are of the form (5.3), where χ and P are given by (4.15) and (4.18). We will thus write

$$\text{③} \sim \Lambda\phi_0^{5/2} \exp\left[\int_s^z \frac{t\phi_0}{5}\, dt\right] \exp\left[-\frac{i}{\epsilon}\int_s^z \frac{1}{\phi_0^2}\, dt\right]. \tag{A.12}$$

Note that in (A.12), we have selected the negative sign (corresponding to ③) and shifted the initial point of integration. However, since $\phi_0 \sim \sqrt{z} - 1/(2z^2) + \cdots$, we see that neither of the integrals in (A.12) converges as $z \to \infty$. Let us therefore write

$$\int_s^z \frac{t\phi_0}{5}\, dt = \int_s^z \frac{t}{5}\left(\phi_0 - \sqrt{t} + \frac{1}{2t^2}\right) dt + \frac{2}{25}\left(z^{5/2} - s^{5/2}\right) - \frac{1}{10}\log\left(\frac{z}{s}\right) \tag{A.13}$$

and

$$\int_s^z \frac{1}{\phi_0^2}\, dt = \int_s^z \left(\frac{1}{\phi_0^2} - \frac{1}{t}\right) dt + \log\left(\frac{z}{s}\right). \tag{A.14}$$

Substituting $z = \epsilon^{-2/5}Z$ into (A.12), (A.13), and (A.14) and expanding the integrals gives the leading-order expression

$$\begin{aligned} \frac{\Lambda s^{1/10} Z^{23/20}}{\epsilon^{23/50}} &\exp\left[\int_s^\infty \frac{t}{5}\left(\phi_0 - \sqrt{t} + \frac{1}{2t^2}\right) dt + \frac{2Z^{5/2}}{25\epsilon} - \frac{2s^{5/2}}{25}\right] \\ &\times \exp\left[\pm\frac{i}{\epsilon}\int_s^\infty \left(\frac{1}{\phi_0^2} - \frac{1}{t}\right) dt \pm \frac{i}{\epsilon}\log\left(\frac{\epsilon^{-2/5}Z}{s}\right) \mp \frac{2i}{5Z^{5/2}}\right]. \end{aligned} \tag{A.15}$$

Copyright © by SIAM. Unauthorized reproduction of this article is prohibited.

This expression gives the inner-to-outer limits of the exponentials. We simply need to match (A.15) with outer-to-inner limit for $A_3 e^{S_3/\epsilon}$. Note from Table 1 that as $Z \to 0$, $S_3' \sim -i/Z + Z^{3/2}/5$, so with A_3 given by (A.2), the third exponential tends to

$$A_3 e^{S_3/\epsilon} \sim \left[\frac{B_3 Z^{23/20}}{(-Z_0)^{1/4}}\right] \exp\left[-\int_{s_1}^{0} \mathcal{G}_3\, dt\right] \exp\left[\frac{2i}{5Z^{5/2}}\right]$$
$$\times \exp\left[\frac{1}{\epsilon}\int_{Z_0}^{0}\left(S_3' + \frac{i}{t}\right) dt - \frac{i}{\epsilon}\log\left(\frac{Z}{Z_0}\right) + \frac{2Z^{5/2}}{25\epsilon} + \cdots\right]. \tag{A.16}$$

Matching (A.15) with (A.16), we find

$$A_3 e^{S_3/\epsilon} \sim \left[\frac{B_3}{(-Z_0)^{1/4}}\right] \exp\left[\frac{1}{\epsilon}\int_{Z_0}^{0}\left(S_3' + \frac{i}{t}\right) dt - \frac{i}{\epsilon}\log\left(\frac{1}{Z_0}\right)\right]$$
$$\times \exp\left[-\int_{s}^{0} \mathcal{G}_3\, dt\right]$$
$$= \left[\frac{\Lambda s^{1/10}}{\epsilon^{23/50}}\right] \exp\left[\int_{s}^{\infty} \frac{t}{5}\left(\phi_0 - t^{1/2} + \frac{1}{2t^2}\right) dt - \frac{2s^{5/2}}{25}\right]$$
$$\times \exp\left[-\frac{i}{\epsilon}\int_{s}^{\infty}\left(\frac{1}{\phi_0^2} - \frac{1}{t}\right) dt - \frac{i}{\epsilon}\log\left(\frac{\epsilon^{-2/5}}{s}\right)\right], \tag{A.17}$$

so that we have

$$\Lambda = \left[\frac{B_3 \epsilon^{23/50}}{(-Z_0)^{1/4} s^{1/10}}\right] \exp\left[-\int_{s}^{\infty} \frac{z}{5}\left(\phi_0 - t^{1/2} + \frac{1}{2t^2}\right) dt + \frac{2s^{5/2}}{25}\right]$$
$$\times \exp\left[-\frac{2i\log\epsilon}{5\epsilon} + \frac{1}{\epsilon}\left\{i\int_{s}^{\infty}\left(\frac{1}{h_0^2} - \frac{1}{t}\right) dt + i\log\left(\frac{Z_0}{s}\right) + \int_{Z_0}^{0}\left(S_3' + \frac{i}{t}\right) dt\right\}\right]$$
$$\times \exp\left(-\int_{s}^{0} \mathcal{G}_3\, dt\right).$$

Finally, writing B_3 in terms of C using (A.11) gives

$$\Lambda = \left[\frac{iC\epsilon^{39/50}}{Z_0^{39/20} s^{1/10}}\right] \exp\left[-\int_{s}^{\infty} \frac{t}{5}\left(\phi_0 - t^{1/2} + \frac{1}{2t^2}\right) dt + \frac{2s^{5/2}}{25} - \frac{2i}{5Z_0^{5/2}}\right]$$
$$\times \exp\left[-\frac{2i\log\epsilon}{5\epsilon} + \frac{1}{\epsilon}\left\{i\int_{s}^{\infty}\left(\frac{1}{\phi_0^2} - \frac{1}{t}\right) dt + i\log\left(\frac{Z_0}{s}\right) + \int_{Z_0}^{0}\left(S_3' - S_1' + \frac{i}{t}\right) dt\right\}\right]$$
$$\times \exp\left[\int_{0}^{Z_0} \left(\mathcal{G}_3 - \mathcal{G}_1\right) dt\right]$$

or simply that

$$\Lambda = \lambda\, \epsilon^{39/50} \exp\left[-\frac{2i\log\epsilon}{5\epsilon} + \frac{b}{\epsilon}\right], \tag{A.18}$$

where b is given by

$$b = i\int_{s}^{\infty}\left(\frac{1}{\phi_0^2} - \frac{1}{t}\right) dt + i\log\left(\frac{Z_0}{s}\right) + \int_{Z_0}^{0}\left(S_3' - S_1' + \frac{i}{t}\right) dt \tag{A.19}$$

Copyright © by SIAM. Unauthorized reproduction of this article is prohibited.

Downloaded 03/12/13 to 163.1.237.161. Redistribution subject to SIAM license or copyright; see http://www.siam.org/journals/ojsa.php

Downloaded 03/12/13 to 163.1.237.161. Redistribution subject to SIAM license or copyright; see http://www.siam.org/journals/ojsa.php

and λ is given by

$$\lambda = \left[\frac{iC}{Z_0^{39/20} s^{1/10}}\right] \exp\left[-\int_s^\infty \frac{t}{5}\left(\phi_0 - t^{1/2} + \frac{1}{2t^2}\right) dt + \frac{2s^{5/2}}{25} - \frac{2i}{5Z_0^{5/2}}\right]$$
$$\times \exp\left[\int_0^{Z_0} (\mathcal{G}_3 - \mathcal{G}_1)\ dt\right]. \tag{A.20}$$

Finally, using the expression in (A.12) with Λ given by (A.18), we have thus derived the previously quoted form of the exponential in (6.15).

Remember that in regards to the selection mechanism, $\mathcal{F}(n, \epsilon)$ in (6.18), we only need the values of $\Psi = \mathrm{Arg}(\lambda)$ and $\Im(b)$. Thus, only the argument of C is required for (A.20), and it is easily verified that $\mathrm{Arg}(C) = \pi$ by comparing the computation of ϕ_0 in section 4 with the asymptotic expansion in (4.3) (adding multiples of 2π to $\mathrm{Arg}(C)$ does not affect the final result). In Appendix B, we will show how the values of S_j' can be computed; once obtained, the above integrals can be easily calculated, and we find that $\Psi \approx -2.7396$ and $\Im(b) \approx -0.1486$.

Appendix B. Computation of Stokes lines and $S_{j,k}(Z)$. The computation of the various complex-valued functions needed to produce Figure 6, as well as the calculation of constants b and Ψ in Appendix A, presents a unique challenge because of the complicated branch structures involved. In this section, we describe how

$$S_{j,k}(Z) = \int_{Z_k}^{Z} S_j'(t)\ dt$$

can be computed for $j = 1, 2, 3$ and $k = 1, 2, \ldots 5$, where S_j' is given by (6.5a, b). Once $S_{j,k}$ is computed, Stokes lines can then be found using (6.12), and b and λ calculated from (A.19) and (A.20). The challenge, however, is in controlling the eventual branch structure of S_j', which involves the composition of complex powers related to its six branch points. Let us illustrate this difficulty with a simple example. Consider the composition

$$(f \circ g)(z), \text{ where } g(z) = z^3 \text{ and } f(z) = z^{1/2}.$$

We thus compute $g(z)$ first, then apply f to $X = g(z)$. If we assume that the branch cuts of X are along the negative real axis, i.e., $\Im[g(z)] = 0$ and $\Re[g(z)] < 0$, then we find that three cuts are required in the original z-plane: ones along rays at $\pm\pi/3$ and π. However, the alternative interpretation of $h(z) = z^{3/2}$ requires only a single cut and gives a much simpler branch structure. The two functions h and $f \circ g$ are clearly not equal, but may still correspond to legitimate analytic continuations. We are free to use whichever one is the simplest, so long as the resultant function has the correct values along the original contour from where we begin the continuation.

Consider now the computation of S_j' in (6.5a, b), which corresponds to analytic continuation from $Z \in \mathbb{R}^+$. We begin by computing β using (6.6) with the branch cuts chosen so that they tend radially outwards from each of the turning points, and with the cut from $Z = 0$ going straight down. Next, $\beta^{1/3}$ is computed with the cut along $\Im[\beta(Z)] = 0$ and $\Re[\beta(Z)] < 0$. This is shown in Figure 8 (left). As we can see, this introduces three new cuts in the Z-plane, coming from the origin. In order to retrieve an alternative definition of $\beta^{1/3}$ which has a simpler branch structure, we proceed along contours with fixed $|Z|$ and encircle the origin. When one of the three

Copyright © by SIAM. Unauthorized reproduction of this article is prohibited.

Downloaded 03/12/13 to 163.1.237.161. Redistribution subject to SIAM license or copyright; see http://www.siam.org/journals/ojsa.php

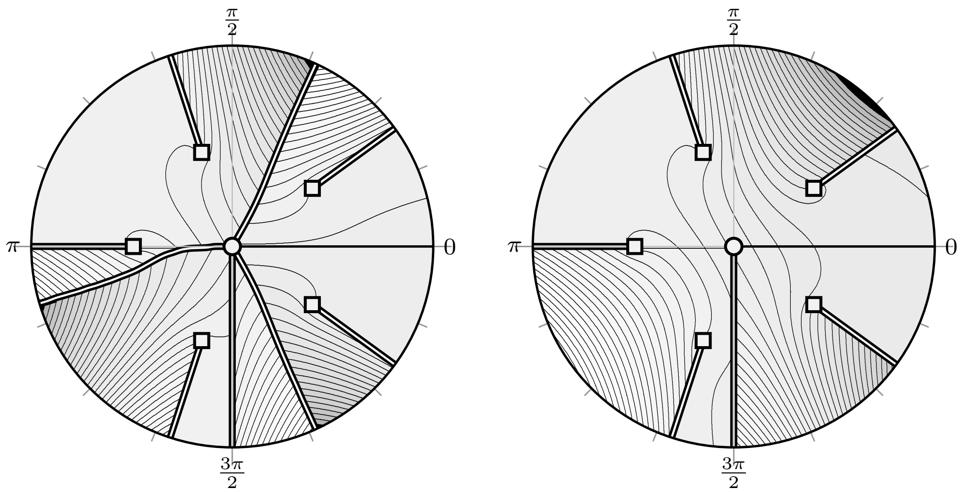

Fig. 8. *Contour plots of* $\Im[\beta^{1/3}(Z)]$ *from* (6.6)*, shown in the complex* Z*-plane with* $0 < |Z| < 2$*. In the left plot, three extraneous branch cuts are visible, while in the right plot they have been removed in favor of a simpler analytic continuation.*

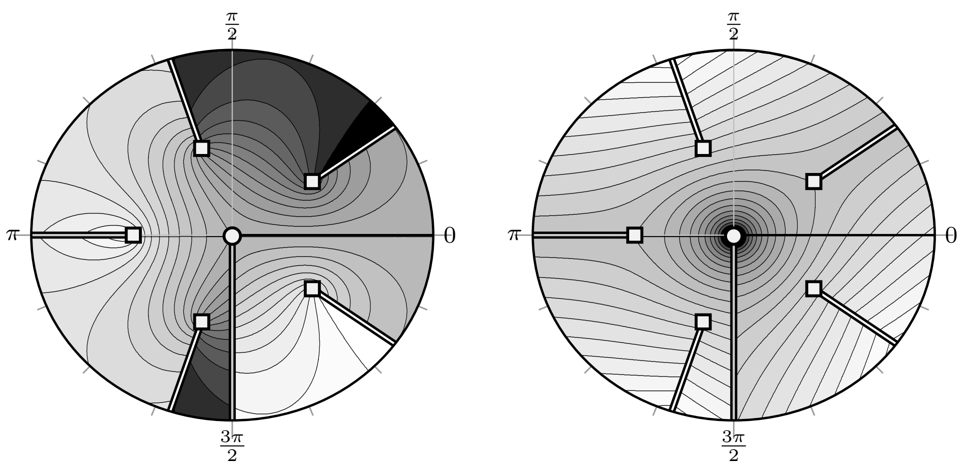

Fig. 9. *(Left) Contour plots of* $\Im[S_1']$ *from* (6.5a)*, and (right)* $\Im[S_{1,0} - S_{3,0}]$ *from* (6.7)*, shown in the complex* Z*-plane with* $0 < |Z| < 2$*. In the right plot, the contour lines from the turning point in the first quadrant form the* $0 > 3$ *and* $3 > 1$ *Stokes lines.*

extraneous cuts is encountered, we thereafter set the argument of $\beta^{1/3}$ to its original value, plus a multiple of $2\pi i/3$. Finally, we verify that this new function is real along $Z \in \mathbb{R}^+$ and is thus the correct analytic continuation. The function is shown in Figure 8 (right). With $\beta^{1/3}$ successfully computed, S_j' follows immediately (shown in Figure 9, left) and, moreover, the integral in (6.7) can be calculated by following radial and angular paths which avoid the existing cuts. A typical result is shown in Figure 9 (right).

Acknowledgments. The authors thank John R. King for very helpful discussions and valuable input. PHT thanks the Oxford Centre for Collaborative and

Copyright © by SIAM. Unauthorized reproduction of this article is prohibited.

Applied Mathematics for their hospitality and support during the final stages of writing.

REFERENCES

[1] A. J. Bernoff, A. L. Bertozzi, and T. P. Witelski, *Axisymmetric surface diffusion: Dynamics and stability of self-similar pinchoff*, J. Statist. Phys., 93 (1998), pp. 725–776.
[2] A. J. Bernoff and T. P. Witelski, *Stability and dynamics of self-similarity in evolution equations*, J. Engrg. Math., 66 (2009), pp. 11–31.
[3] J. P. Boyd, *Weakly Nonlocal Solitary Waves and Beyond-All-Orders Asymptotics*, Kluwer Academic, Dordrecht, The Netherlands, 1998.
[4] J. P. Boyd, *The Devil's invention: Asymptotics, superasymptotics and hyperasymptotics*, Acta Appl., 56 (1999), pp. 1–98.
[5] M. P. Brenner, J. R. Lister, and H. A. Stone, *Pinching threads, singularities and the number* 0.0304..., Phys. Fluids, 8 (1996), pp. 2827–2836.
[6] S. J. Chapman, *On the role of Stokes lines in the selection of Saffman-Taylor fingers with small surface tension*, European J. Appl. Math., 10 (1999), pp. 513–534.
[7] S. J. Chapman, B. J. Hunton, and J. R. Ockendon, *Vortices and boundaries*, Quart. J. Appl. Math., 56 (1998), pp. 507–5129.
[8] S. J. Chapman, J. R. King, and K. L. Adams, *Exponential asymptotics and Stokes lines in nonlinear ordinary differential equations*, R. Soc. Lond. Proc. Ser. A Math. Phys. Eng. Sci., 454 (1998), pp. 2733–2755.
[9] S. J. Chapman and J.-M. Vanden-Broeck, *Exponential asymptotics and capillary waves*, SIAM J. Appl. Math., 62 (2002), pp. 1872–1898.
[10] R. Combescot, V. Hakim, T. Dombre, Y. Pomeau, and A. Pumir, *Shape selection of Saffman-Taylor fingers*, Phys. Rev. A, 56 (1986), pp. 2036–2039.
[11] R. Combescot, V. Hakim, T. Dombre, Y. Pomeau, and A. Pumir, *Analytic theory of the Saffman-Taylor fingers*, Phys. Rev. A, 37 (1988), pp. 1270–1283.
[12] O. Costin and R. D. Costin, *On the formation of singularities of solutions of nonlinear differential systems in antistokes directions*, Invent. Math., 145 (2001), pp. 425–485.
[13] O. Costin and S. Tanveer, *Complex singularity analysis for a nonlinear PDE*, Comm. Partial Differential Equations, 31 (2006), pp. 593–637.
[14] R. B. Dingle, *Asymptotic Expansions: Their Derivation and Interpretation*, Academic Press, London, 1973.
[15] J. Eggers, *Nonlinear dynamics and breakup of free-surface flows*, Rev. Modern Phys., 69 (1997), pp. 865–929.
[16] J. Eggers and M. A. Fontelos, *The role of self-similarity in singularities of partial differential equations*, Nonlinearity, 22 (2009), pp. R1–R44.
[17] J. Eggers and E. Villermaux, *Physics of liquid jets*, Rep. Progr. Phys., 71 (2008), 036601.
[18] R. Grimshaw, *Exponential asymptotics and generalized solitary waves*, in Asymptotic Methods in Fluid Mechanics: Survey and Recent Advances, Springer, Wien, New York, 2010, pp. 71–120.
[19] M. D. Kruskal and H. Segur, *Asymptotics beyond all orders in a model of crystal growth*, Stud. Appl. Math., 85 (1991), pp. 129–181.
[20] T. G. Myers, *Thin films with high surface tension*, SIAM Rev., 40 (1998), pp. 441–462.
[21] A. B. Olde Daalhuis, *On the computation of Stokes multipliers via hyperasymptotics. Resurgent functions and convolution integral equations*, Sūrikaisekikenkyūsho Kōkyūroku, (1999), pp. 68–78.
[22] A. B. Olde Daalhuis, S. J. Chapman, J. R. King, J. R. Ockendon, and R. H. Tew, *Stokes phenomenon and matched asymptotic expansions*, SIAM J. Appl. Math., 55 (1995), pp. 1469–1483.
[23] A. Oron, S. H. Davis, and S. G. Bankoff, *Long-scale evolution of thin liquid films*, Rev. Modern Phys., 69 (1997), pp. 931–980.
[24] G. G. Stokes, *On the discontinuity of arbitrary constants which appear in divergent developments*, Trans. Camb. Phil. Soc., 10 (1864), pp. 106–128.
[25] G. G. Stokes, *On the discontinuity of arbitrary constants that appear as multiples of semi-convergent series*, Acta. Math. Stockholm, 26 (1902), pp. 393–397.
[26] S. Tanveer and X. Xie, *Analyticity and nonexistence of classical steady Hele-Shaw fingers*, Comm. Pure Appl. Math., 56 (2003), pp. 353–402.
[27] P. H. Trinh, *Exponential asymptotics and Stokes line smoothing for generalized solitary waves*, in Asymptotic Methods in Fluid Mechanics: Survey and Recent Advances, Springer, Wien, New York, 2010, pp. 121–126.

Downloaded 03/12/13 to 163.1.237.161. Redistribution subject to SIAM license or copyright; see http://www.siam.org/journals/ojsa.php

Copyright © by SIAM. Unauthorized reproduction of this article is prohibited.

Downloaded 03/12/13 to 163.1.237.161. Redistribution subject to SIAM license or copyright; see http://www.siam.org/journals/ojsa.php

[28] P. H. Trinh, S. J. Chapman, and J.-M. Vanden-Broeck, *Do waveless ships exist? Results for single-cornered hulls*, J. Fluid Mech., 685 (2011), pp. 413–439.

[29] D. Vaynblat, J. R. Lister, and T. P. Witelski, *Rupture of thin viscous films by van der Waals forces: Evolution and self-similarity*, Phys. Fluids, 13 (2001), pp. 1130–1140.

[30] D. Vaynblat, J. R. Lister, and T. P. Witelski, *Symmetry and self-similarity in rupture and pinchoff: A geometric bifurcation*, European J. Appl. Math., 12 (2001), pp. 209–232.

[31] R. B. White, *Asymptotic Analysis of Differential Equations*, Imperial College Press, London, 2005.

[32] M. B. Williams and S. H. Davis, *Nonlinear theory of film rupture*, J. Colloid Interface Sci., 90 (1982), pp. 220–228.

[33] T. P. Witelski and A. J. Bernoff, *Stability of self-similar solutions for van der Waals driven thin film rupture*, Phys. Fluids, 11 (1999), pp. 2443–2445.

[34] X. Xie and S. Tanveer, *Analyticity and nonexistence of classical steady Hele-Shaw fingers*, Comm. Pure Appl. Math., 56 (2002), pp. 353–402.

[35] W. W. Zhang and J. R. Lister, *Similarity solutions for van der Waals rupture of a thin film on a solid substrate*, Phys. Fluids, 11 (1999), pp. 2454–2462.

Copyright © by SIAM. Unauthorized reproduction of this article is prohibited.